Journal of Organometallic Chemistry, 435 (1992) 9–20
Elsevier Sequoia S.A., Lausanne
JOM 22708

Synthesis and solution properties of the boron-containing clusters $HM_4(CO)_{12}BAu_2(dppf)$ (M = Fe or Ru) and the competitive formation of $\{HM_4(CO)_{12}BHAu\}_2(dppf)$ for M = Ru (dppf = 1,1′-bis(diphenylphosphino)ferrocene). Molecular structure of $HRu_4(CO)_{12}BAu_2(dppf) \cdot 2\ CHCl_3$

Sylvia M. Draper and Catherine E. Housecroft
University Chemical Laboratory, Lensfield Road, Cambridge CB2 1EW (UK)

and Arnold L. Rheingold
Department of Chemistry, University of Delaware, Newark, DE 19716 (USA)

(Received January 14, 1992)

Abstract

The reaction of $[PPN][HM_4(CO)_{12}BH]$ (M = Fe or Ru) with ClAu(dppf)AuCl (dppf = 1,1′-bis(diphenylphosphino)ferrocene) leads to $HM_4(CO)_{12}BAu_2(dppf)$ in which the environment of the boron atom depends upon the identity of M. For M = Ru, the boron atom is interstitial, with the hydride ligand wholly associated with the tetraruthenium framework. For M = Fe, an isomer equilibrium exists in solution between a metallaborane and a metallaboride cluster with the former, $Fe_4(CO)_{12}BHAu_2(dppf)$ (**1**) being the dominant species. The difference in structure is attributed to the increase in size of the tetrametal butterfly framework from Fe_4 to Ru_4 and follows the pattern previously noted for $HM_4(CO)_{12}BAu_2(PPh_3)_2$. For M = Ru, the formation of $HRu_4(CO)_{12}BAu_2(dppf)$ (**3**) competes with that of the linked bicluster $\{HRu_4(CO)_{12}BHAu\}_2(dppf)$ (**2**). A crystallographic structural determination of **3** has revealed that the hexametal skeleton in **3** encapsulates the boron atom but is non-octahedral. The two Au atoms are related by a molecular C_2 axis and each bridges one $B-Ru_{wingtip}$ edge. The orientation of the ferrocenyl group with respect to the cluster core is controlled by the location of the gold atoms and the two C_5 rings are locked in an approximately mutually eclipsed position. In solution, ^1H NMR spectroscopy in the Cp region has been used to study the fluxional behaviour of **3**; three processes are mutually dependent (i) a "rocking" motion of the two Au atoms with respect to the Ru_4B core (ii) inversion at the phosphorus atoms (iii) cyclopentadienyl ring twisting.

Introduction

Over the past few years we have presented detailed studies of the family of compounds of general formula $HFe_4(CO)_{12}BAu_2L_2$ (L = monodentate phosphine

Correspondence to: Dr. C.E. Housecroft or Dr. A.L. Rheingold.

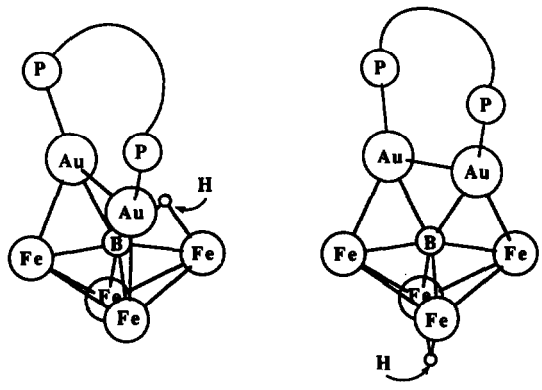

1 **1**

isomer A **isomer B**

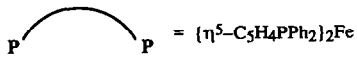

Fe = $Fe(CO)_3$

or arsine) [1–5] and have shown that the geometry of the Fe_4BAu_2 core is controlled by the steric requirements of the ligand L and that the site of the hydride ligand is dependent upon the Fe_4BAu_2 array (structures **A** and **B**) [3,4,6*]. Retaining a common L and changing the group 8 transition metal from Fe to Ru also has the effect of altering the cluster core geometry as we have demonstrated in a comparison of the structures of $HM_4(CO)_{12}BAu_2(PPh_3)_2$ (M = Fe or Ru) [1,2,7].

A large number of transition metal clusters incorporating gold(I) phosphine ligands is now known [8] and it has been observed that the AuL fragments are often labile on the cluster surface. For example, in Ru_3Au_2 clusters structural evidence suggests that interconversion between trigonal bipyramidal and square based pyramidal structures occurs *via* a Berry-type mechanism [9]. In $HFe_4(CO)_{12}BAu_2L_2$, we have observed that for compounds of structural type **A** the two phosphorus atoms, which are in different environments in the solid state, exchange in solution. We have proposed that the exchange occurs *via* an intramolecular "rocking" of the $\{Au_2L_2\}$ unit across the top of the Fe_4B cluster core [2,10]. The AuL units in compounds of type **B** are related by a C_2 axis [6*] and are equivalent both in the solid state and in solution. However, the observation of a single ^{31}P NMR resonance in solution does not preclude the possibility of synchronised movement of the two AuL units across the plane that cuts through the boron, the two butterfly wing-tip and the hinge-bridging hydride atoms. Such a motion would effectively convert one enantiomer of the chiral cluster $HFe_4(CO)_{12}BAu_2L_2$ into the other and similarly for ruthenium analogues.

* Reference number with asterisk indicates a note in the list of references.

A ligand that has received increased attention of late is 1,1'-bis(diphenylphosphino)ferrocene (abbreviated to dppf). The structure of the free ligand has been determined and shows a *trans*-arrangement of the PPh_2 groups [11]. The ligand may coordinate through the phosphorus donors to either one or two metal atoms. The two cyclopentadienyl rings are free to twist with respect to one another and a range of conformations is observed in solid state structures [12–25]. Here we report the results of an investigation of the reaction of ClAu(dppf)AuCl [19,26] with $[HM_4(CO)_{12}BH]^-$ (M = Fe or Ru). The aims of this work were twofold. Firstly we wished to investigate the possibility that the {Au(dppf)Au} group may act as a linkage between two $\{HM_4(CO)_{12}BH\}$ cluster fragments as well as or instead of reacting to produce the digold cluster $HM_4(CO)_{12}BAu_2(dppf)$. Secondly, we considered that if $HM_4(CO)_{12}BAu_2(dppf)$ were formed, ^1H NMR spectral data for the cyclopentadienyl moiety could provide an insight into fluxional behaviour in solution.

Experimental section

General data

FT-NMR spectra were recorded on a Bruker WM 250 or AM 400 spectrometer. ^1H NMR shifts are reported with respect to δ 0 for Me_4Si; ^{11}B NMR with respect to δ 0 for $F_3B \cdot OEt_2$; ^{31}P NMR with respect to δ 0 for H_3PO_4. All downfield chemical shifts are positive. Infrared spectra were recorded on a Perkin–Elmer FT 1710 spectrophotometer. FAB mass spectra were recorded on a Kratos MS 890 instrument.

All reactions were carried out under argon by standard Schlenk techniques. Solvents were dried over suitable reagents and freshly distilled under dinitrogen before use. Separations were carried out by t.l.c. with Kieselgel 60-PF-254 (Merck). $HAuCl_4 \cdot 3H_2O$ and dppf (Aldrich) were used as received. [PPN][$HM_4(CO)_{12}BH$] (M = Fe [27] or M = Ru [7]) were prepared as previously reported.

Preparation of ClAu(dppf)AuCl

During these investigations, the synthesis and structure of ClAu(dppf)AuCl were reported [19]. We present here our method of synthesis of this compound. A solution of $HAuCl_4 \cdot 3H_2O$ (0.79 g, 2 mmol) in ethanol (15 mL) was added to a solution of dppf (1.11 g, 2 mmol) in THF (15 mL). The mixture was stirred at room temperature for 1.5 h until it had produced a yellow precipitate. The supernatant liquid was removed and the solid was dried under vacuum before being recrystallised from CH_2Cl_2 and pentane at 0°C. ClAu(dppf)AuCl was collected as orange needle-like crystals in 70% yield (m.p. 259–263°C). Elemental analyses and spectroscopic data agree with those published [19,26].

Preparation of $Fe_4(CO)_{12}BHAu_2(dppf)$, 1

[PPN][$HFe_4(CO)_{12}BH$] (0.28 g, 0.25 mmol) was dissolved in CH_2Cl_2 (20 mL) and the resulting red-brown solution was added to solid ClAu(dppf)AuCl (0.23 g, 0.25 mmol) and $TlPF_6$ (0.02 g, 0.06 mmol). The mixture was stirred at room temperature for 1 h; no colour change was observed. The mixture was filtered, the filtrate collected and solvent removed. Crude products were redissolved in the minimum volume of CH_2Cl_2 and were separated chromatographically by eluting

with CH_2Cl_2 : hexane (3 : 1). Compound **1** was collected as the third (lime green) fraction in ≈ 20% yield. The first and fourth bands to be eluted were $Fe_3(CO)_{12}$ and [PPN][$HFe_3(CO)_{11}$] while the second fraction remains uncharacterised at present [28*]. **1**: 250-MHz ^{1}H NMR (CD_2Cl_2, 292 K) δ 7.6–7.3 (m, *Ph*), 4.60 (v. br, *Cp*), 4.16 (br, *Cp*), −10.4 (br, Fe–*H*–*B*, see text); 128-MHz ^{11}B NMR (CD_2Cl_2, 298 K) δ +144.5; 162-MHz ^{31}P NMR (CD_2Cl_2, 298 K) δ +45.3; IR (CH_2Cl_2, cm^{-1}) ν(CO) 2157 w, 2127 w, 2058 m, 2020 vs, 1996 vs, 1888 w, 1840 w; FAB-MS in 3-NBA matrix, *m/z* 1522 (P^+, simulated and observed isotopic distributions agree).

Reaction of [PPN][$HRu_4(CO)_{12}BH$] with ClAu(dppf)AuCl

CH_2Cl_2 (20 mL) was added to solid [PPN][$HRu_4(CO)_{12}BH$] (0.11 g, 0.08 mmol), ClAu(dppf)AuCl (0.08 g, 0.08 mmol) and $TlPF_6$ (0.02 g, 0.06 mmol). The mixture was stirred at room temperature for 45 min and the solution deepened in colour to dark orange. The mixture was filtered, the filtrate collected and solvent removed. Crude products were redissolved in the minimum volume of CH_2Cl_2 and were separated by TLC by eluting with CH_2Cl_2 : hexane (1 : 1). The first fraction (yellow, yield ≈ 10%) to be eluted was $H_4Ru_4(CO)_{12}$. The second (yellow, yield ≈ 30%) and third (orange, yield ≈ 40%) bands were identified as {$HRu_4(CO)_{12}BHAu$}$_2$(dppf), **2**, and $HRu_4(CO)_{12}BAu_2$(dppf), **3**, respectively. **2**: 250-MHz ^{1}H NMR ($CDCl_3$, 298 K) δ 7.7–7.3 (m, 20H, *Ph*), 4.75 (s, 4H, *Cp*), 4.20 (s, 4H, *Cp*), −4.7 (br, Ru–*H*–B), −20.8 (s, Ru–*H*–Ru); 128-MHz ^{11}B NMR ($CDCl_3$, 298 K) δ +133.5; 162-MHz ^{31}P NMR ($CDCl_3$, 298 K) δ +48.0; IR (CH_2Cl_2, cm^{-1}) ν(CO) 2081 m, 2067 s, 2051 s, 2029 m, 2011 m; FAB-MS in 3-NBA matrix, *m/z* 1706 (P^+–{$HRu_4(CO)_{12}BH$}, simulated and observed isotopic distributions agree); no parent ion observed. **3**: 250-MHz ^{1}H NMR (CD_2Cl_2, 298 K) δ 7.7–7.4 (m, 20H, *Ph*), 4.67 (broad, see text, *Cp*), 4.07 (s, 4H, *Cp*), −20.9 (br, Ru–*H*–Ru); 128-MHz ^{11}B NMR (CD_2Cl_2, 298 K) δ +166.2; 162-MHz ^{31}P NMR (CD_2Cl_2, 298 K) δ +42.8; IR (CH_2Cl_2, cm^{-1}) ν(CO) 2069 m, 2038 s, 2024 vs, 2015 wsh, 1990 m, 1952 w; FAB-MS in 3-NBA matrix, *m/z* 1701 (P^+, simulated and observed isotopic distributions agree).

Crystal structure determination

Crystallographic data are collected in Table 1. An orange-red crystal was grown from $CHCl_3$ layered with hexane. The crystal was affixed to a glass fibre with epoxy cement. Photographic techniques showed 2/*m* Laue symmetry, and systematic absences in the diffraction data limited the choice of space group to either *C*2/*c* or *Cc*. The former, centrosymmetric, space group was initially chosen due to the potential presence of a two-fold rotational axis in the molecules passing through Fe, B and the midpoints of the Au–Au(*) and Ru(1)–Ru(1*) bonds. This axis was found, subsequently, to be aligned with the crystallographic *b* axis, and the positions of these atoms were fixed accordingly. The remainder of the molecule was constructed from a series of difference maps and found to refine to a chemically reasonable final result. This was taken as an indication of the correctness of the original centrosymmetric assignment.

The structure was corrected for absorption by a numerical procedure which obtains an empirical absorption tensor from an expression relating F_o and F_c

Table 1

Crystal data for $HRu_4(CO)_{12}BAu_2(dppf)\cdot 2\,CHCl_3$, **3**

(a) *Crystal parameters*			
formula	$C_{48}H_{31}Au_2BCl_6FeO_{12}P_2Ru_4$	Z	4
formula weight	1939.29	cryst. dimens., mm	0.20×0.32×0.38
cryst. system	monoclinic	cryst. colour	orange-red
space group	$C2/c$	V, Å^3	5723.3(20)
a, Å	16.819(3)	D(calc), g cm^{-3}	2.250
b, Å	12.998(2)	μ(Mo-K_α), cm^{-1}	67.48
c, Å	26.993(6)	temp, K	296
β, deg	104.11(2)	T(max)/T(min)	4.667
(b) *Data collection*			
diffractometer	Nicolet R3m	rflns. collected	4818
monochromator	graphite	indpt. rflns.	4486
radiation	Mo-K_α	indpt. obsvd. rflns.	3137 (5σ)
2θ scan range, deg	4–45	std. rflns.	3std/197 rflns
data collected (h, k, l)	±19, +14, +30	var. in stds, %	≈ 6
(c) *Refinement*			
$R(F)$, %	6.96	$\Delta(\rho)$, e Å^{-3}	1.853
$R_w(F)$, %	7.53	N_o/N_v	9.9
Δ/σ(max)	0.048	GOF	1.650

(H. Hope, B. Moezzi, Department of Chemistry, University of California, Davis). A correction was also applied for an approximate 6% decay in reflection intensity.

The structure was solved by direct methods. The phenyl rings (but not the Cp rings) were refined as rigid, planar bodies. All non-hydrogen atoms were refined with anisotropic thermal parameters. All computations used the SHELXTL program library (G. Sheldrick, Nicolet (Siemens, Madison, WI)).

Supplementary data are deposited with the Cambridge Crystallographic Data Centre.

Results and discussion

The {Au(dppf)Au} unit as a cluster bridge or a bicluster linkage

The reaction of ClAu(dppf)AuCl with [PPN][$HFe_4(CO)_{12}BH$] proceeds to give several products but only one that incorporates the {Au(dppf)Au} unit. The ^{1}H and ^{11}B NMR spectral characteristics of this product, **1**, are similar to those of $Fe_4(CO)_{12}BHAu_2L_2$ in which L = PPh_3, [1,2], $P(C_6H_4$-2-Me$)_3$, [4] $P(c$-$C_6H_{11})_3$, [4] PEt_3, [3,4] or PPh_2Me [4]. We therefore formulate **1** as $Fe_4(CO)_{12}BHAu_2$(dppf) with the bidentate dppf ligand taking the place of the two monodentate ligands in $Fe_4(CO)_{12}BHAu_2L_2$. The ^{1}H NMR spectrum in the highfield region exhibits a broad signal at δ −10.4 and the ^{11}B NMR resonance at δ +144.5 sharpens upon proton decoupling. Both sets of data are consistent with the presence of an Fe–H–B bridging hydrogen atom as shown in structure **1**, isomer **A**. The presence in solution of a second isomer of type **B** is evidenced by the fact that over the temperature range 298 K to 202 K, the resonance in the ^{1}H NMR spectrum at δ −10.4 shifts to −9.5 and, in concert with this change, a sharp signal at δ −24.9

assigned to an Fe–H–Fe bridging hydride ligand appears. These results indicate that the ratio of isomers **A**:**B** in dichloromethane solution is $\approx 92:8$ [4]. By comparison with other related tetrairon systems that we have studied, this result indicates that the steric requirements of the {Au(dppf)Au} fragment are similar to those of two $\{AuPEt_3\}$ fragments [3,4].

The reaction of ClAu(dppf)AuCl with $[PPN][HRu_4(CO)_{12}BH]$ occurs *via* two competitive pathways to generate two products, **2** and **3**, which contain the {Au(dppf)Au} moiety. Compound **3** is related to **1** and has the formulation $HRu_4(CO)_{12}BAu_2(dppf)$; the {Au(dppf)Au} unit bridges over the top of a single cluster. At room temperature in the highfield region of the ^1H NMR spectrum, the spectral signature of **3** differs from that of **1** in that the observed resonance is typical of an Ru–H–Ru bridging hydride (δ −20.9) rather than indicating the presence of a boron-attached hydrogen atom. This is consistent with **3** adopting a structure akin to **1**, but solely in the form of isomer **B** and this is confirmed in the crystallographic study presented below.

Product **2** is characterised at 298 K in the ^1H NMR spectrum by resonances assigned to Ph and Cp protons and by two highfield resonances, one broad at δ −4.7 and one sharp at δ −20.8 assigned to Ru–H–B and Ru–H–Ru hydrides respectively. The ^{11}B NMR spectral resonance at δ +133.5 sharpens upon proton decoupling. The ^{11}B and highfield ^1H NMR spectroscopic properties are reminiscent of a cluster containing an $\{HRu_4(CO)_{12}BHAu\}$ moiety [29]. Two cluster products are feasible: neutral $\{HRu_4(CO)_{12}BHAu\}_2(dppf)$ or ionic $[\{HRu_4(CO)_{12}BH\}_2Au][(dppf)_2Au]$. We have recently reported the preparation and structural characterisation of $[\{HRu_4(CO)_{12}BH\}_2Au][PPN]$ [29]. We propose that **2** is the neutral {Au(dppf)Au} linked bicluster $\{HRu_4(CO)_{12}BHAu\}_2(dppf)$ (Fig. 1). A neutral rather than ionic product is implied by the fact that **2** is soluble in hexane. Further, the ^{31}P NMR chemical shift data for LAuCl, $[L_2Au]^+$ and $HM_4(CO)_{12}BAu_2L_2$ show a trend [1–4,30–32] and the presence of cluster bound gold(I) phosphine as opposed to the cation is apparent from a consideration of the ^{31}P NMR spectral shift. The shift of δ +48.0 in **2** is similar to that of δ +42.8 observed in **3** in which the presence of cluster bound {Au(dppf)Au} moiety has been confirmed crystallographically (see below). Were **2** to contain the $[(dppf)_2Au]^+$ cation, a signal at $\delta \approx +22$ should be observed [26].

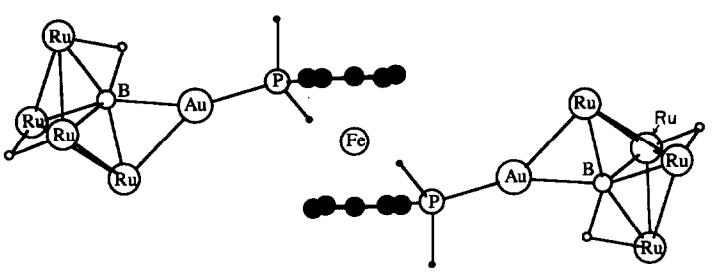

Fig. 1. Proposed structure of **2**.

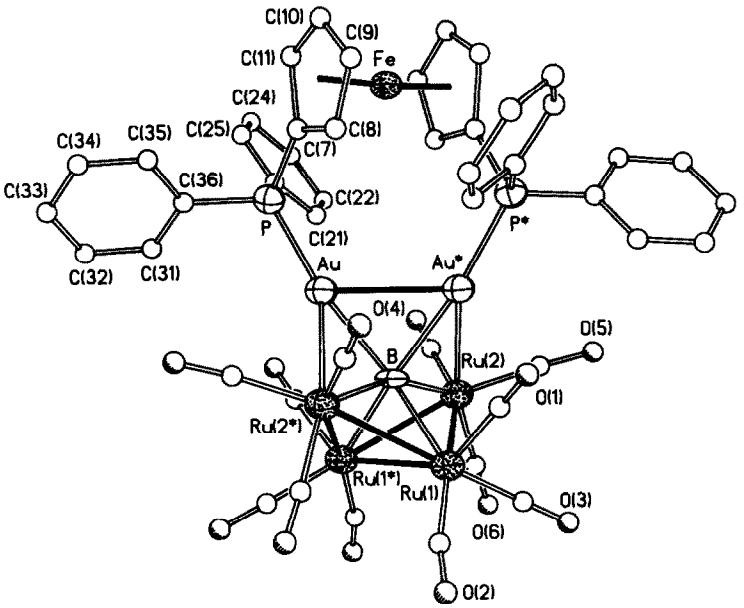

Fig. 2. Molecular structure of **3** showing atomic labelling scheme.

Molecular structure of $HRu_4(CO)_{12}BAu_2(dppf)$, 3

The molecular structure of **3** is given in Fig. 2 atomic coordinates and thermal parameters in Table 2 and selected bond lengths and angles in Table 3. The six metal atoms encapsulate the boron atom rendering it interstitial although the geometry of the Ru_4Au_2 core is non-octahedral; the Au–Au(*) vector lies at 46° to the Ru(1)–Ru(1*) vector. The molecule possesses a C_2 axis and thus the structure of **3** is more closely related to that observed for the cluster $HFe_4(CO)_{12}BAu_2(PEt_3)_2$ (isomer **B**) [3,4] than to that of $HRu_4(CO)_{12}BAu_2(PPh_3)_2$, the core-structure of which lies on a pathway between isomers **A** and **B** with ruthenium replacing iron atoms [7]. The increased symmetry noted in going from $HRu_4(CO)_{12}BAu_2(PPh_3)_2$ to **3** is attributed to the smaller steric requirements of the dppf ligand compared to two triphenylphosphine ligands.

The geometry of the $\{Ru_4B\}$ cluster core in **3** may be compared to those in the parent butterfly $HRu_4(CO)_{12}BH_2$ [33] and in $HRu_4(CO)_{12}BAu_2(PPh_3)_2$ [7]. One characteristic parameter is the internal dihedral angle of the Ru_4 butterfly; this varies little being 118° in $HRu_4(CO)_{12}BH_2$ [33], 117.4(1)° in $HRu_4(CO)_{12}BAu_2(PPh_3)_2$ [7], and 116.5(1)° in **3**. The boron atom is pulled slightly further out of the Ru_4 framework in **3** (0.419(3) Å) compared to its position in $HRu_4(CO)_{12}BH_2$ (0.39 Å) [33,34] and $HRu_4(CO)_{12}BAu_2(PPh_3)_2$ (0.37(1) Å) [7]. The butterfly hinge in **3** is longer than the Ru_{hinge}–Ru_{wing} edges and this is in accord with the trend observed in $HRu_4(CO)_{12}BH_2$ [33], $HRu_4(CO)_{12}BAu_2(PPh_3)_2$ [7] and $[\{HRu_4(CO)_{12}BH\}_2Au]^-$ [29]. In each of the latter three compounds, the hinge is bridged by a hydride ligand. ^1H NMR spectroscopic data and an inspection of the orientations of the carbonyl ligands attached to atoms Ru(1) and Ru(1*) indicate that this edge is similarly bridged by a hydrogen atom in **3**.

Table 2

Atomic coordinates ($\times 10^4$) and isotropic thermal parameters ($Å^2 \times 10^3$) for $HRu_4(CO)_{12}BAu_2$-(dppf)·2 $CHCl_3$, **3**

	x	y	z	U_{eq} [a]
Au	339.0(5)	5819.8(6)	7071.3(3)	57.8(3)
Ru(1)	308.3(11)	8528.7(13)	8049.3(7)	57.6(6)
Ru(2)	−1202.0(10)	7533.0(13)	7587.2(7)	59.0(6)
Fe	0	2590(3)	7500	55(1)
P	211(3)	4331(4)	6598(2)	58(2)
B	0	7211(19)	7500	46(10)
O(1)	1056(13)	7091(12)	8925(6)	94(8)
O(2)	1555(12)	10230(13)	8467(7)	97(8)
O(3)	−871(12)	9519(18)	8583(7)	108(9)
O(4)	−2429(11)	6324(14)	6799(7)	94(8)
O(5)	−1803(12)	6869(17)	8512(8)	112(10)
O(6)	−2275(11)	9462(16)	7451(8)	101(9)
C(1)	736(15)	7589(28)	8607(10)	103(13)
C(2)	1179(15)	9580(19)	8291(9)	71(9)
C(3)	−475(15)	9149(17)	8359(9)	70(9)
C(4)	−1987(15)	6808(20)	7089(10)	79(10)
C(5)	−1557(15)	7087(17)	8154(11)	81(10)
C(6)	−1870(13)	8757(15)	7494(10)	66(9)
C(7)	589(12)	3268(15)	7005(8)	55(7)
C(8)	1064(13)	3348(15)	7505(9)	62(8)
C(9)	1259(13)	2339(18)	7713(9)	66(8)
C(10)	875(13)	1654(15)	7325(8)	61(8)
C(11)	441(13)	2119(12)	6904(9)	58(8)
C(21)	−1477(9)	4509(10)	6302(5)	67(8)
C(22)	−2266	4205	6047	122(17)
C(23)	−2376	3369	5713	94(12)
C(24)	−1697	2837	5634	94(12)
C(25)	−908	3141	5889	68(9)
C(26)	−798	3977	6223	52(7)
C(31)	582(11)	5090(13)	5746(7)	105(14)
C(32)	1013	5157	5366	139(19)
C(33)	1681	4512	5381	92(13)
C(34)	1919	3800	5776	149(21)
C(35)	1489	3732	6156	101(13)
C(36)	821	4377	6141	57(7)
C(s)	817(6)	8405(7)	9999(4)	198(22) [b]
Cl(1)	1094(9)	9411(11)	9656(4)	184(7)
Cl(2)	860(11)	8808(12)	10616(4)	222(10)
Cl(3)	−172(8)	8016(12)	9709(4)	194(8)

[a] Equivalent isotropic U defined as one third of the trace of the orthogonalized U_{ij} tensor. [b] U_{iso}.

The ferrocenyl unit in **3** lies directly over the boron atom with the iron atom lying on the C_2 axis that also passes through the boron atom and the midpoint of Ru(1)–Ru(1*). The mode of coordination of the dppf ligand, *i.e.* bridging over two adjacent transition metal atoms, has only once previously been confirmed crystallographically: in $Ru_3(CO)_{10}$(dppf) [22], the dppf ligand bridges one edge of an Ru_3 triangle and the two cyclopentadienyl rings are tilted by 5.4° [22] from being coparallel and are twisted by ≈ 72° with respect to one another [35*]. This twisting means that the C_5 rings themselves are virtually eclipsed but the C–P

Table 3

Selected bond distances (Å) and bond angles (deg) in $HRu_4(CO)_{12}BAu_2(dppf)\cdot 2\,CHCl_3$, **3**

(a) *Bond distances*			
Au–P	2.300(6)	Au–B	2.292(20)
Au–Au(*)	2.818(2)	Au–Ru(2*)	2.695(2)
Ru(1)–Ru(2)	2.853(2)	Ru(1)–B	2.242(19)
Ru(1)–Ru(1*)	2.893(3)	Ru(1)–Ru(2*)	2.854(3)
Ru(2)–B	2.133(5)	Ru(2)–Au(*)	2.695(2)
Ru(2)–Ru(1*)	2.854(3)	B–Au(*)	2.292(20)
B–Ru(1*)	2.242(19)	B–Ru(2*)	2.133(5)
P–C(7)	1.782(20)	Fe–C(7)	2.046(22)
Fe–C(8)	2.040(21)	Fe–C(9)	2.080(21)
Fe–C(10)	2.051(23)	Fe–C(11)	2.024(25)
(b) *Bond angles*			
P–Au–B	160.6(2)	P–Au–Au(*)	117.0(2)
B–Au–Au(*)	52.1(4)	P–Au–Ru(2*)	148.8(2)
B–Au–Ru(2*)	49.8(3)	Au(*)–Au–Ru(2*)	90.6(1)
Ru(2)–Ru(1)–B	47.7(1)	Ru(2)–Ru(1)–Ru(1*)	59.6(1)
B–Ru(1)–Ru(1*)	49.8(4)	Ru(2)–Ru(1)–Ru(2*)	94.3(1)
B–Ru(1)–Ru(2*)	47.6(1)	Ru(1*)–Ru(1)–Ru(2*)	59.5(1)
Ru(1)–Ru(2)–B	51.0(5)	Ru(1)–Ru(2)–Au(*)	83.0(1)
B–Ru(2)–Au(*)	55.2(6)	Ru(1)–Ru(2)–Ru(1*)	60.9(1)
Au–B–Ru(1)	152.9(1)	Au(*)–Ru(2)–Ru(1*)	105.2(1)
Au–P–C(7)	109.8(7)	Au–B–Ru(2)	124.7(7)
Au–B–Au(*)	75.9(8)	Ru(1)–B–Au(*)	108.3(1)
Ru(2)–B–Au(*)	74.9(3)	Ru(1)–B–Ru(1*)	80.4(8)
Ru(2)–B–Ru(1*)	81.4(6)	Ru(2)–B–Ru(2*)	157.4(13)

bonds diverge from one another. In **3**, the C_5 rings are also slightly tilted with respect to each other; $\angle Cp_{centroid}–Fe–Cp_{centroid} = 176.0(5)°$. They deviate by 8° from being eclipsed but the rings are mutually twisted so that the C–P vectors deviate from one another by 80°. Ring twisting and tilting are two degrees of freedom by which the dppf ligand is able to modify its conformation and adjust its bite angle in compounds in which it chelates to a metal atom [36*].

In **3**, the Au–Au separation is 2.818(2) Å while in $Ru_3(CO)_{10}(dppf)$, the ligand bridges an Ru–Ru edge of length 2.928 Å [22]. Our results illustrate that the dppf ligand is able to bridge a dimetal distance smaller than the 2.93 Å found in $Ru_3(CO)_{10}(dppf)$ and thus, the particularly long Ru–Ru distance observed in the latter may not be a consequence [22] of the restricted flexibility of the dppf ligand. We liken the behaviour of the $\{M_2(dppf)\}$ framework to a spiral concertina that may be stretched or shortened in accord with variations in the M–M separation. Further structural data are required before one can make meaningful comments upon the variations in geometrical features of the $\{M_2(dppf)\}$ frame since there are several mutually dependent parameters *e.g.* the distances M–P, M–M, P · · · P and Fe–X (where X = midpoint of the M–M bond), the twist and tilt angles of the Cp rings and the angle subtended by the M–M vector and a line joining the centroids of the two Cp rings.

Solution properties of 3

The solid state structure of **3** shows that the two $Au\{Ph_2PC_5H_4\}$ groups are equivalent. The cyclopentadienyl ring orientations are such that there are four Cp

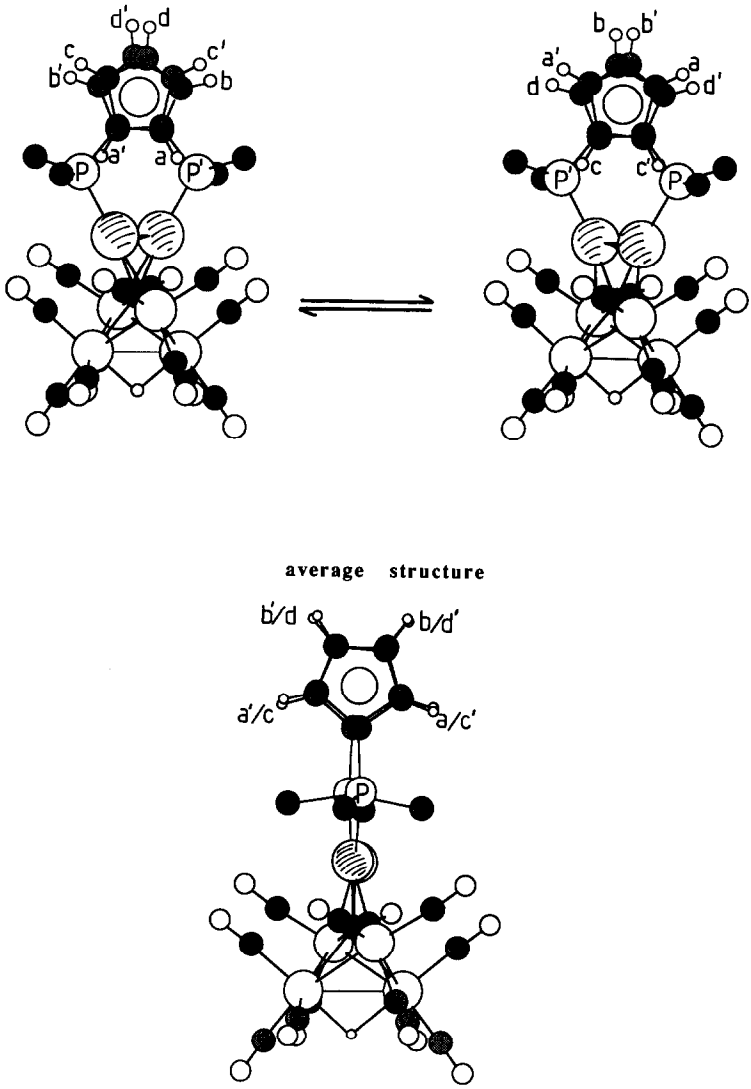

Fig. 3. Schematic representation of the interconversion of the two enantiomers of **3** which may be interchanged *via* inversion at the two phosphorus atoms. Atoms attached to the back Cp ring are labelled with primes. The intermediate structure has the two $\{C_5P\}$ moieties in eclipsed positions.

proton environments labelled *a* to *d* in the top left hand part of Fig. 3. Figure 4 illustrates that at 298 K, only two resonances are observed in the Cp region of the ^{1}H NMR spectrum of **3** and one signal is considerably broader than the other. As the temperature is lowered, the two resonances collapse and at 215 K, four signals are frozen out, one being at significantly lower field (δ 5.37) than the other three (δ 4.38, 3.94, 3.72). We assign the resonance at δ 5.37 to protons *a* which face in towards the Au_2P_2 cavity, (Fig. 3, top left). Compound **3** is a chiral molecule, and the variable temperature ^{1}H NMR spectroscopic data may be interpreted in terms of the fluxional process illustrated in Fig. 3 that interconverts the two enantiomers.

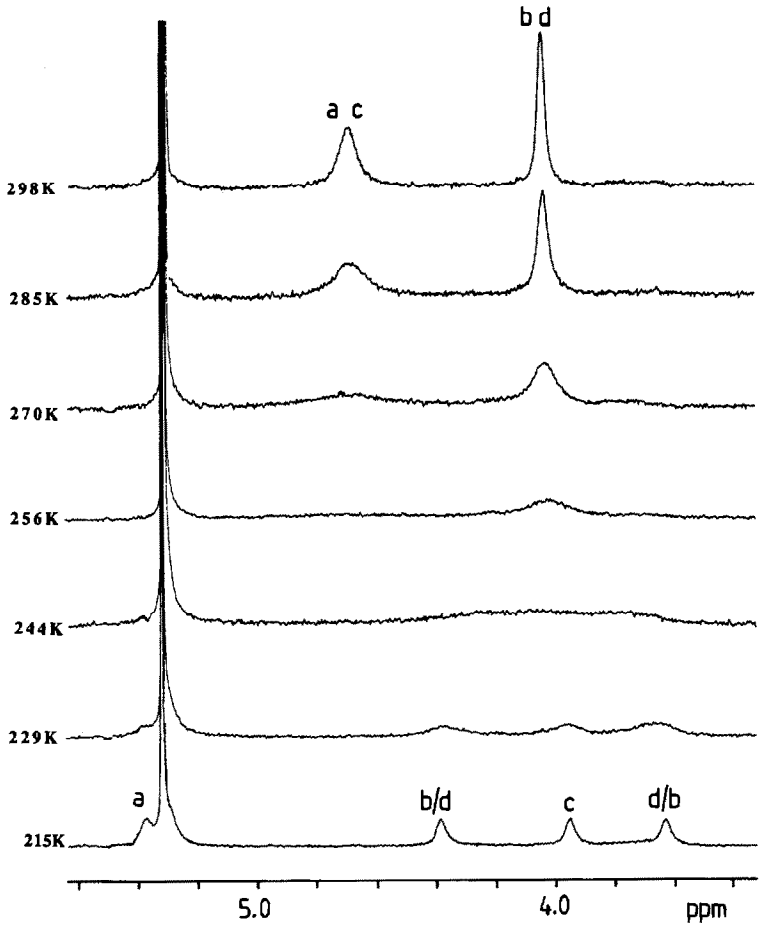

Fig. 4. Variable temperature 250-MHz ^{1}H NMR spectrum of **3** in CD_2Cl_2 plotted in the Cp region.

The process involves inversion at the two phosphorus atoms and concomitant twisting of the two cyclopentadienyl rings. This motion must be in concert with each gold atom moving from one side of the Ru_4B butterfly to the other, and the process exchanges the positions of protons *a* and *c*, and *b* and *d*. The average structure observed at room temperature is schematically represented at the bottom of Fig. 3 and exhibits eclipsed $\{PC_5H_5\}$ units. The fact that we are able to observe this fluxional process in **3** underlines one of the advantages of the dppf ligand in site labelling in the ^{1}H NMR spectrum.

Acknowledgments

We thank the donors of the Petroleum Research Fund, administered by the American Chemical Society for their support (Grant #22771-AC3), the S.E.R.C. for a studentship (to S.M.D.) and the NSF for a Grant (CHE 9007852) towards the purchase of a diffractometer at the University of Delaware. Johnson-Matthey is thanked for generous loans of $RuCl_3$. The assistance of Helen Larcombe in preliminary studies of the synthesis of ClAu(dppf)AuCl is gratefully acknowledged.

References and notes

1 C.E. Housecroft and A.L. Rheingold, J. Am. Chem. Soc., 108 (1986) 6420.
2 C.E. Housecroft and A.L. Rheingold, Organometallics, 6 (1987) 1332.
3 C.E. Housecroft, A.L. Rheingold and M.S. Shongwe, Organometallics, 7 (1988) 1885.
4 C.E. Housecroft, A.L. Rheingold and M.S. Shongwe, Organometallics, 8 (1989) 2651.
5 C.E. Housecroft, A.L. Rheingold, M.S. Shongwe and P. Zanello, J. Organomet. Chem., 408 (1991) 7.
6 Structures **A** and **B** are the extreme geometries observed for the M_4BAu_2 core. Some deviations may occur, *e.g.* in $HRu_4(CO)_{12}BAu_2(PPh_3)_2$ where the structure approximates to isomer **B** but does not possess a C_2 axis (ref. 7).
7 A.K. Chipperfield, C.E. Housecroft and A.L. Rheingold, Organometallics, 9 (1990) 681.
8 I.D. Salter, Adv. Organomet. Chem., 29 (1989) 249.
9 A.G. Orpen and I.M. Salter, Organometallics, 10 (1991) 111.
10 K.S. Harpp and C.E. Housecroft, J. Organomet. Chem., 340 (1988) 389.
11 U. Casellato, D. Ajo, G. Valle, B. Corain, B. Longato and R. Grazani, J. Crystallogr. Spectrosc., 18 (1988) 583.
12 T. Hayashi, M. Konishi, Y. Kobori, M. Kumada, T. Higuchi and K. Hirotsu, J. Am. Chem. Soc., 106 (1984) 158.
13 I.R. Butler, W.R. Cullen, T.-J. Kim, S.J. Rettig and J. Trotter, Organometallics, 4 (1985) 972.
14 D.A. Clemente, G. Pilloni, B. Corain, B. Longato and M. Tiripichio-Camellini, Inorg. Chim. Acta, 115 (1986) L9.
15 S. Onaka, Bull. Chem. Soc. Jpn., 59 (1986) 2359.
16 T. Hayashi, M. Kumada, T. Higuchi and K. Hirotsu, J. Organomet. Chem., 334 (1987) 195.
17 M.I. Bruce, I.R. Butler, W.R. Cullen, G.A. Houtsantonis, M.R. Snow, and R.T. Tiekink, Aust. J. Chem., 41 (1988) 963.
18 T.M. Miller, K.J. Ahmed and M.S. Wrighton, Inorg. Chem., 28 (1989) 2347.
19 T.H. Hill, G.R. Girard, F.L. McCabe, R.K. Johnson, P.D. Stupik, J.H. Zhang, W.M. Reiff and D.S. Eggleston, Inorg. Chem., 28 (1989) 3529.
20 T.-J. Kim, K.-H. Kwon, S.-C. Kwon, J.-O. Baeg, S.-C. Shim and D.-H. Lee, J. Organomet. Chem., 389 (1990) 205.
21 C.E. Housecroft, S.M. Owen, P.R. Raithby and B.A.M. Shaykh, Organometallics, 9 (1990) 1617.
22 S.T. Chacon, W.R. Cullen, M.I. Bruce, O.B. Shawkataly, F.W.B. Einstein, R.H. Jones and A.C. Willis, Can. J. Chem., 68 (1990) 2001.
23 A. Togni, S.D. Pastor and G. Rihs, J. Organomet. Chem., 381 (1990) C21.
24 B. Longato, G. Pilloni, R. Grazani and U. Casellato, J. Organomet. Chem., 407 (1991) 369.
25 B.S. Haggerty, C.E. Housecroft, A.L. Rheingold and B.A.M. Shaykh, J. Chem. Soc., Dalton Trans., (1991) 2175.
26 A. Houlton, R.M.G. Roberts, J. Silver and R.V. Parish, J. Organomet. Chem., 418 (1991) 269.
27 C.E. Housecroft, M.L. Buhl, G.J. Long and T.P. Fehlner, J. Am. Chem. Soc., 109 (1987) 3323.
28 The use of centrifugal chromatography (Kieselgel 60-PF-254 mesh from Merck; eluent CH_2Cl_2: hexane, 1:1) in place of TLC allowed the separation of a fifth, air-sensitive product in moderate yield. The compound is a PPN salt, but we have, as yet, been unable to characterise it fully; it exhibits a signal in the ^{11}B NMR spectrum at δ +90.4 and the IR spectrum (CH_2Cl_2) is characterised in the ν(CO) region by absorptions at 2014 s, 2005 s, 1988 vs. The dppf ligand is not retained.
29 S.M. Draper, C.E. Housecroft, J.E. Rees, M.S. Shongwe, B.S. Haggerty and A.L. Rheingold, Organometallics, in press.
30 E.L. Muetterties, W.G. Peet, P.A. Wegner and C.W. Alegranti, Inorg. Chem., 9 (1970) 2447.
31 R.V. Parish, O. Parry and C.A. McAuliffe, J. Chem. Soc., Dalton Trans., (1981) 2098 and references therein.
32 S.J. Verners-Price, M.A. Mazid and P.J. Sadler, J. Chem. Soc., Dalton Trans., (1984) 969 and references therein.
33 F.-E. Hong, D.A. McCarthy, J.P. White III, C.E. Cottrell and S.G. Shore, Inorg. Chem., 29 (1990) 2874.
34 C.E. Housecroft, Adv. Organomet. Chem., 33 (1991) 1.
35 Determined by us using crystallographic coordinates for $Ru_3(CO)_{10}$(dppf) from ref. 22.
36 See for example ref. 21 and references therein.